

Document downloaded from:

<http://hdl.handle.net/10251/179797>

This paper must be cited as:

Nguyen, D.; Zvanovec, S.; Bohata, J.; Ortega Tamarit, B.; Vallejo-Castro, L.; Ghassemlooy, Z. (2020). On N-PAM and M-QAM implementation within the hybrid RoF-FSO-PON system. IEEE. 1-4. <https://doi.org/10.1109/WASOWC49739.2020.9410197>



The final publication is available at

<https://doi.org/10.1109/WASOWC49739.2020.9410197>

Copyright IEEE

Additional Information

© 2020 IEEE. Personal use of this material is permitted. Permission from IEEE must be obtained for all other uses, in any current or future media, including reprinting/republishing this material for advertising or promotional purposes, creating new collective works, for resale or redistribution to servers or lists, or reuse of any copyrighted component of this work in other works.

On N -PAM and M -QAM implementation within the hybrid RoF-FSO-PON system

Dong-Nhat Nguyen

Department of Electromagnetic Field
Czech Technical University in Prague
Prague, Czech Republic
dongnhat@fel.cvut.cz

Stanislav Zvanovec

Department of Electromagnetic Field
Czech Technical University in Prague
Prague, Czech Republic
xzvanove@fel.cvut.cz

Jan Bohata

Department of Electromagnetic Field
Czech Technical University in Prague
Prague, Czech Republic
bohataj2@fel.cvut.cz

Beatriz Ortega

Instituto de Telecomunicaciones y
Aplicaciones Multimedia, ITEAM
Universitat Politècnica de València
Valencia, Spain
bortega@dcom.upv.es

Luis Vallejo

Instituto de Telecomunicaciones y
Aplicaciones Multimedia, ITEAM
Universitat Politècnica de València
Valencia, Spain
luivalc2@iteam.upv.es

Zabih Ghassemlooy

Faculty of Engineering and
Environment
Northumbria University
Newcastle upon Tyne, United Kingdom
z.ghassemlooy@northumbria.ac.uk

Abstract—This paper investigates an optical transmission architecture of a passive optical network (PON), which is compatible with the millimeter-wave radio-over-fiber and free-space optics systems (RoF-FSO) under weak-to-strong atmospheric turbulence (AT) regimes to enable seamless connectivity as part of next-generation broadband wireless access networks. We first analyze and evaluate in simulation the transmission performance of the integrated system at 40 GHz for 10 Gb/s N -pulse amplitude modulation (N -PAM) with $N = 2, 4$. Link performance shows that, 4-PAM outperforms 2-PAM in terms of tolerance to the combined impairment of fiber chromatic dispersion and AT. We then experimentally demonstrate the proof-of-concept integrated RoF-FSO-PON at 25 GHz using 20 MHz M -quadrature amplitude modulation (M -QAM) signals with $M = 4, 16, 64$. We show that, for QAM with a higher-order M , the link performance is being more affected by the combined impairments.

Keywords—radio-over-fiber, free-space optics, passive optical networks, turbulence, millimeter-wave

I. INTRODUCTION

Future broadband wireless access (BWA) networks will need to support multi-gigabit bandwidth-intensive applications as high-speed services have been rapidly increasing. Due to the limited available bandwidth and spectrum congestion particularly at frequencies below 6 GHz in the current BWA schemes, it is, therefore, challenging to transmit higher data rates R_b over long transmission distances with high quality of service (QoS). Thus, shifting to higher carrier frequencies i.e., in the millimeter-wave (MMW) bands, is the most obvious option in order to overcome spectral congestion and achieve higher data transmission rates [1].

Radio-over-fiber (RoF) systems operating in the MMW bands (e.g., within 24 – 60 GHz) take full advantage of broadband and lightwave features of optical fiber (OF) such as single-mode fiber (SMF) and multi-mode fiber (MMF) [2], [3]. They have been identified as potential candidates to extend the transmission range and offer higher R_b e.g., by distributing the MMW signal from the central station (CS) to the remote base station (BS) or in convergent optical and BWA networks [4]. MMW signals can be photonically generated by different techniques, among others, by using optical heterodyning or external modulation [3], [5]. Approaches employing a Mach-Zehnder modulator (MZM)

at different bias point allow obtaining modulation schemes such as double sideband, single sideband and optical carrier suppression (OCS) [4]. Recent literature reports a number of schemes using MZMs e.g., a 60 GHz MMW signal was used for 2 Gb/s data transmission using two cascaded MZMs over a 21 km of SMF [6], a 24 Gb/s carrier-less amplitude and phase modulated signal over 40 GHz MMW along 40 km of SMF and a 1.5 m of wireless link [7] and a 25 GHz MMW over a 50 km of SMF and 40 m of wireless link [3].

Free-space optics (FSO) transmission technology has been recognized as a suitable low-cost alternative for emergency communication network deployment [8]. This is due to the fact that OF-based telecommunications infrastructures can be severely damaged due to e.g., natural disasters. Additionally, the installation of OF cables particularly in an urban area is expensive and time-consuming. FSO can also be used for transmission of radio frequency (RF) signals as part of the last mile BWA networks to deliver high-quality broadband wireless services to e.g. rural communities and remote areas; the concept is best known as radio over free space optics (RoFSO), which is standardized by International Telecommunication Union [8]. Commercial FSO systems operating at 10 Gb/s over a transmission range of a few kilometers are readily available in the market [9] and can be adopted as part of the hybrid platform. In [10], a digital terrestrial television broadcasting RF signal was successfully transmitted over a 1 km FSO turbulent link at a wavelength of 1550 nm. The transmission of long-term evolution (LTE) signal operating at a carrier frequency of 2.6 GHz over a 2 m FSO link under various atmospheric turbulence (AT) levels for cloud radio access network applications was experimentally demonstrated in [11].

In this work, we first propose and examine in simulation a combination scheme of RoF and RoFSO operating at 40 GHz MMW (within the recommended frequency band for fifth-generation (5G) network [12]), denoted as RoF-FSO. The proposed scheme is highly attractive for future BWA networks since it offers higher R_b and increases the level of flexibility as well as the coverage range. In addition, this scheme can be integrated with passive optical networks (PON) to enable seamless high-speed (> 10 Gb/s) connections [13]. Note that, the most common standardized

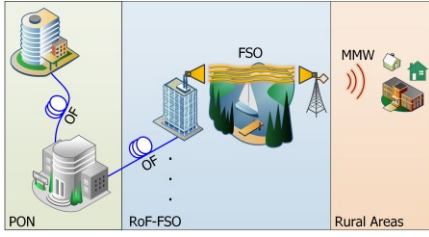


Figure 1. The simplified concept of delivering RF signal over hybrid RoF-FSO-PON systems to rural areas.

intensity-modulation and direct-detection (IM/DD) PON system uses non-return-to-zero signal also known as 2-pulse amplitude modulation (2-PAM) with R_b up to 10 Gb/s as reported in [14]. Quadrature amplitude modulation (QAM) signal (i.e., 5 Gb/s 16-QAM) has also been recently considered as an attractive candidate in PON since they offer a number of advantages such as high spectral efficiency and high tolerance to fiber chromatic dispersion (CD) [15]. Although there are no current standards for 4-PAM based RoF-FSO, it has been reported that 4-PAM will be widely utilized in next-generation PON systems [14] since it doubles R_b and reduces the bandwidth requirements for optical and electrical devices. We then experimentally demonstrate a proof-of-concept RoF-FSO-PON at 25 GHz using 20 MHz M -quadrature amplitude modulation (QAM) signals with $M = 4, 16, 64$. In the proposed hybrid link, the propagating signal experiences degradation due to the cumulative impairment of CD and AT, which leads to pulse spreading (i.e., intersymbol interference). These detrimental effects are also investigated. Fig. 1 illustrates the deployment scenario of the proposed hybrid link to deliver BWA to the rural and underserved areas, where high-speed Internet connectivity is unavailable.

II. SIMULATION SETUP AND RESULTS USING N -PAM SIGNALS

A. Setup

Fig. 2 illustrates the schematic block diagram of the simulation setup for the proposed hybrid RoF-FSO-PON link. First, at the optical line terminal (OLT), a 10 Gb/s 2-PAM input data stream is generated and applied to the pre-emphasis module (i.e., a raised cosine filter with a roll-off factor of 0.5) in order to increase the system bandwidth. The 2-PAM signal is applied to MZM1 for external modulation of a continuous wave laser beam at a wavelength and output power of 1550 nm and 6 dBm, respectively. The modulated optical signal is then transmitted over a 30 km SMF (representing PON). Next, the output of SMF is applied to MZM2 in order to generate the MMW-OCS signal based on frequency doubling at the CS. MZM2 is biased at V_{π} of 4 V and is driven by a 20 GHz local oscillator (LO) (i.e., RF sinusoidal clock). Note that MZMs have an insertion loss of 5 dB. The up-converted optical MMW signal is then amplified using an erbium-doped fiber amplifier (EDFA) to a power level of ~ 2.5 dBm prior to transmission over the optical distribution network (ODN) which consists of the standard SMF and FSO link spans of 10 km and 500 m, respectively. The FSO link in this case represents the last mile BWA connection. Two AT levels are considered: 5×10^{-15} and $5 \times 10^{-12} \text{ m}^{-2/3}$ which represent weak and strong AT in a practical outdoor environment, respectively. Both FSO

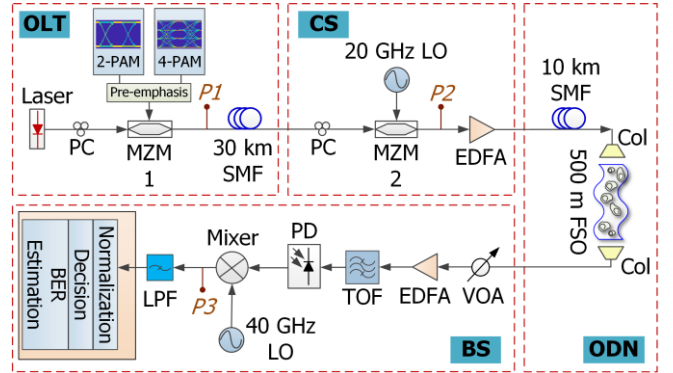


Figure 2. Simulation setup of the proposed hybrid RoF-FSO-PON link using N -PAM signals. Col: collimator.

collimators have an aperture diameter of 2.54 cm as employed in our previous experiment [3]. The optical signal is transmitted to a variable optical attenuator (VOA) in order to adjust the received optical power P_r level before launching to an optically pre-amplified receiver (Rx) which consists of an erbium doped fiber amplifier (EDFA) that has a gain and noise figure of 20 dBm and 5 dB, respectively, a tunable optical filter (TOF) with a bandwidth of 60 GHz to suppress the out-of-band noise (i.e., the amplified spontaneous noise of EDFA) and a PIN photodetector (PD) that has a responsivity and dark current of 0.75 A/W and 10 nA, respectively. The output of the PD can be wirelessly distributed to the end users using e.g., 40 GHz horn antennas [7]. However, since the main aim is to assess hybrid RoF-FSO-PON link, the regenerated electrical MMW signal is down-converted to the baseband using a mixer and a 40 GHz LO. The demodulated signal is then passed through a 4th order Bessel low pass filter (LPF) with a bandwidth of 7.5 GHz. Finally, the output of the LPF is post-processed in MATLAB to determine the BER.

B. Results

1) Performance Evaluation of 10 Gb/s 2-PAM Signal

We evaluate the performance of the 10 Gb/s N -PAM hybrid RoF-FSO-PON link for the following scenarios as illustrated in Fig. 2:

- i. Back-to-back (B2B): no ODN section in the hybrid transmission which is used as a benchmark
- ii. Hybrid link (no FSO): only SMF included in the ODN
- iii. Hybrid link: both SMF and FSO included in the ODN with FSO channel affected by weak and strong AT regimes

First, we examine the 2-PAM transmission performance. Fig. 3 (a) and (b) illustrate optical spectra for 10 Gb/s 2-PAM and double-sideband with optical carrier suppression (OCS) scheme at locations P_1 , P_2 in Fig. 2, respectively. For 2-PAM, the spectrum displays a peak at a wavelength of 1550 nm and null-to-null bandwidth of 20 GHz (measured at the power level of ~ 40 dBm). Whereas Fig. 3(b) shows two peaks at the wavelength of 1549.84 nm and 1550.16 nm with much reduced power levels of -20 dBm, and separated by 40 GHz with a carrier suppression ratio (CSR) of ~ 35 dB. Fig. 3(c) displays the spectrum of the down-converted RF signal at point P_3 in Fig. 2, showing the recovered 40 GHz

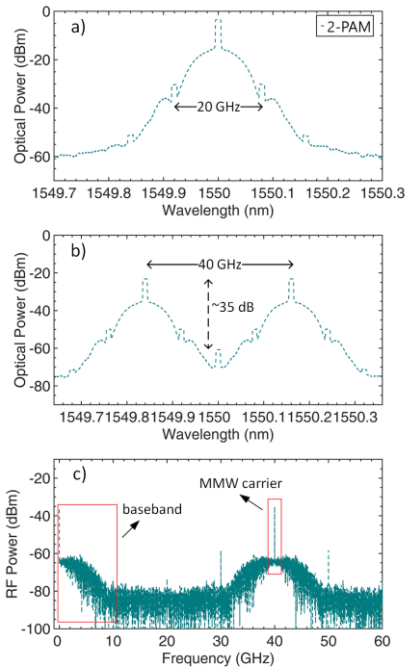


Figure 3. Observed spectra at different points in Fig. 2: (a) 10 Gb/s 2-PAM optical signal at $P1$, (b) optical MMW double-sideband with OCS at $P2$ and (c) RF signal at $P3$.

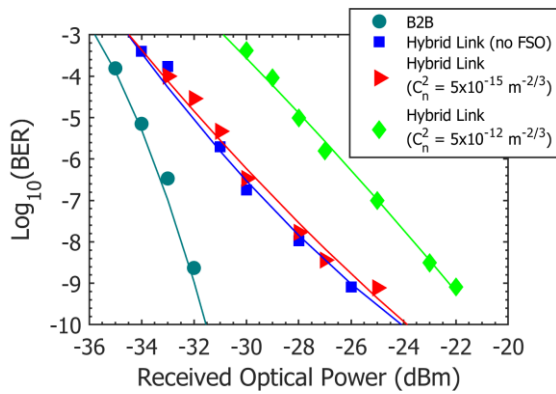


Figure 4. BER against P_r for 10 Gb/s 2-PAM under different scenarios.

carrier and the baseband components.

Fig. 4 depicts the BER as a function of the received optical power P_r for 10 Gb/s 2-PAM with the aforementioned scenarios. At a BER of 10^{-9} , the P_r is about -32 dBm for the B2B and it increases by 6 dB for the hybrid link (no FSO). For the hybrid link with the FSO channel under weak and strong AT regimes, the optical power penalties are 6.2 and 10.5 dB, respectively, compared to the B2B link. In addition, we notice up to two orders of magnitude deterioration in the BER performance at the P_r of -25 dBm under weak and strong AT levels, respectively.

2) Performance Evaluation of 10 Gb/s 4-PAM Signal

Here, we use the same setup as shown in Fig. 2. The electrical 4-PAM signal is generated using two 5 Gb/s 2-PAM signals, which are then combined to produce an equally spaced 4-PAM signal. Note, (i) one of the electrical 2-PAM data streams is delayed by 24-bit using an electrical delay line to ensure that the two 2-PAM signals can be de-correlated; and (ii) the second 2-PAM data is 6-dB attenuated using an

electrical attenuator. For 4-PAM the total average BER defined for the three decision threshold levels is given by [16]:

$$BER_{\text{total}} = BER_{\text{Low}} + 2BER_{\text{Middle}} + BER_{\text{Top}} \quad (1)$$

Fig. 5 (a), (b) and (c) illustrate the optical and RF spectra at different locations in Fig. 2 when a 10 Gb/s 4-PAM signal is transmitted. Note, for 4-PAM the spectrum as illustrated in Fig. 5(a) shows a peak at 1550 nm with a null-to-null bandwidth of 10 GHz. The resulting spectral efficiency of 1 b/s/Hz (i.e., twice that of 2-PAM) is achieved. However, the main disadvantage of 4-PAM is the increased BER compared to the 2-PAM for the same P_r . This is due to multi-levels, which are more susceptible to noise [16]. Fig. 6 depicts the BER performance against P_r for the 10 Gb/s 4-PAM B2B signal transmission, where the inset shows the corresponding eye diagram. As shown, the best BER performance is observed for the low eye pattern (i.e., intensity levels of “0” and “1”) followed by the middle (levels “1” and “2”) and top eye (levels “2” and “3”). More specifically, at a BER of 10^{-9} the power penalties are 1.7 and 4 dB for the middle and top modulation levels, respectively compared with the low level. The top eye shows the worst case due to the noise source (i.e., thermal and shot noise from the detector).

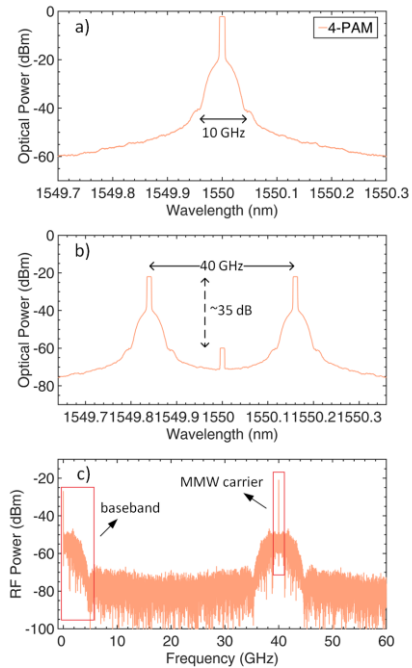


Figure 5. Observed spectra at different points in Fig. 2: (a) 10 Gb/s 4-PAM optical signal at $P1$, (b) optical MMW double-sideband with OCS at $P2$ and (c) RF signal at $P3$.

The aggregate BER performance against P_r for 10 Gb/s 4-PAM for B2B and hybrid links, calculated by using Eq. (1), is shown in Fig. 7. At a BER of 10^{-9} the Rx sensitivity for B2B is about -24 dBm, which is 8 dB higher than 10 Gb/s 2-PAM, as shown in Fig. 4, due to the additional levels of 4-PAM. However, unlike 2-PAM, the 4-PAM exhibits better performance with only ~1 dB power penalty after the hybrid link (no FSO) compared to 6 dB for the 10 Gb/s 2-PAM system. For the hybrid link with FSO channel under weak and strong AT regimes, the optical power penalties are low (i.e., about 1 and 2.5 dB at a BER of 10^{-9} , respectively) in

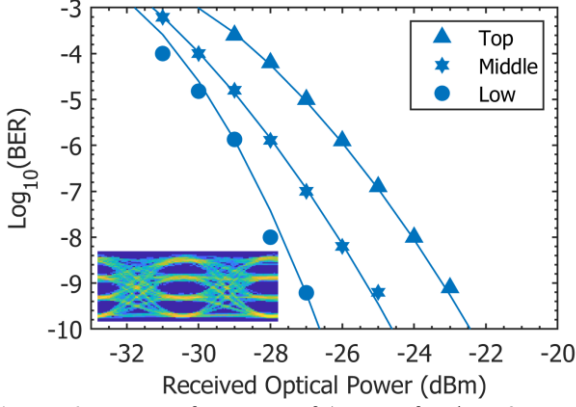


Figure 6. BER performance of 4-PAM for the B2B scenario at 10 Gb/s for each eye pattern (top, middle and low). Inset shows the corresponding eye diagram at a BER of 10^{-9} .

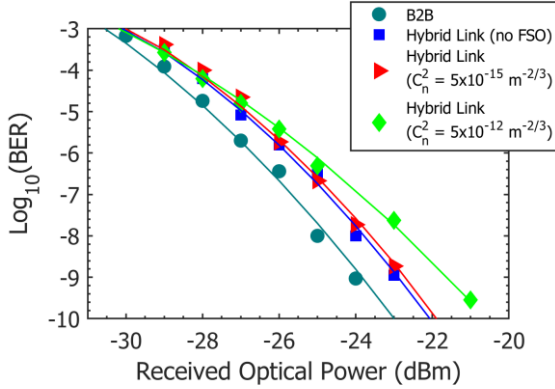


Figure 7. BER against P_r for 10 Gb/s 4-PAM under different scenarios.

comparison to the B2B. 4-PAM clearly displays reduced optical power penalties than 2-PAM. In addition, at the P_r of -25 dBm we observe that less than one order of magnitude downgrade in the BER performance when comparing between weak and strong AT conditions. 4-PAM is therefore found to be more tolerant to the aggregate impairment of CD and AT compared to 2-PAM.

Although, the B2B Rx sensitivity of 4-PAM is degraded when comparing to 2-PAM but on the other hand, 4-PAM is capable to double the bit rate and spectral efficiency since its symbol rate is half of 2-PAM. It is worth mentioning that the optical sensitivity improvement for 4-PAM can be simply achieved by optimizing the level spacing or extinction ratio of the signal at the transmitter. Also note that, using an avalanche photo-detector instead of the PIN detector at the Rx can further enhance the sensitivity by a few dBs [17].

III. EXPERIMENTAL SETUP AND RESULTS USING M -QAM SIGNALS

In this section, we experimentally demonstrate a proof-of-concept hybrid RoF-FSO-PON link at 25 GHz using 20 MHz M -QAM signals.

A. Setup

The experimental setup is depicted in Fig. 8, which is closely similar to the simulation setup in Fig. 2.

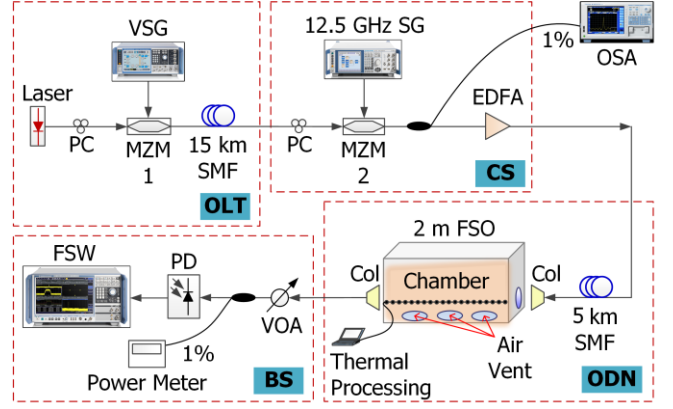


Figure 8. Experimental setup of the proposed hybrid RoF-FSO-PON link using M -QAM signals. VSG: vector signal generator and SG: signal generator.

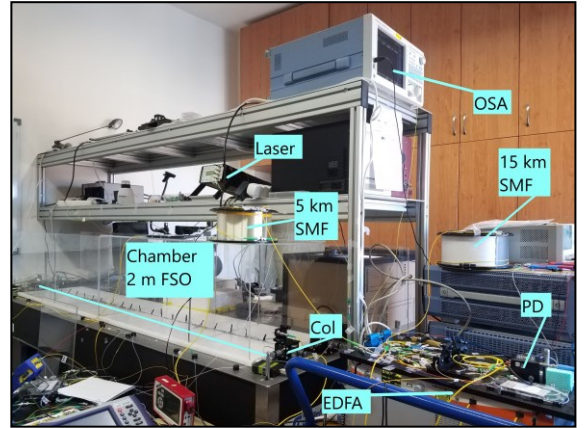


Figure 9. Photo of the experimental testbed.

A vector signal generator (R&S SMW 200A) was used to generate 20 MHz M -QAM signals. Note, this testbed (see Fig. 9) focused at 25 GHz, which is also a recommended frequency for 5G network [12]. The SMF length of the PON is 15 km while the SMF length in ODN is 5 km. The FSO channel is 2 m, which is constructed within the lab-made chamber. The AT level is determined about $6 \times 10^{-14} \text{ m}^{-2/3}$. Detail of our FSO chamber and AT measurements can be found in [3]. The BS is simplified with only a single PD Rx instead of the optically pre-amplified Rx as in simulation. The 20 MHz 4/16/64-QAM signals are directly evaluated at 25 GHz using a signal and spectrum analyzer (R&S FSW).

B. Results

Fig. 10 shows the measured error vector magnitude (EVM) as a function of P_r for 20 MHz M -QAM signals after the hybrid RoF-FSO-PON link transmission, respectively. Also shown in Fig. 10 are the 17.5%, 12.5% and 8% EVM required limits for 4-, 16- and 64-QAM signals, respectively according to the third-generation partnership project (3GPP) specifications [18]. As can be seen, a good quality of the recovered M -QAM signals is achieved (see insets in Fig. 10) which confirms the feasibility of our proposed hybrid system. Fig. 11 shows the corresponding BER performance. At a BER of 10^{-9} the Rx sensitivity of 4/16/64-QAM signals is about 0, 3 and 5 dBm which results in the power penalty of 2 and 4 dB when comparing 4- to 16- and 64-QAM, respectively.

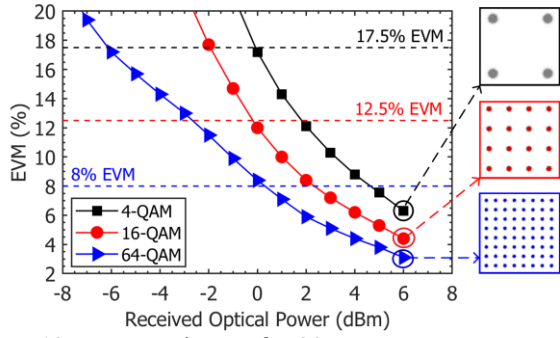


Figure 10. EVM against P_r for 20 MHz M -QAM. Insets are the corresponding M -QAM constellations at P_r of 6 dBm.

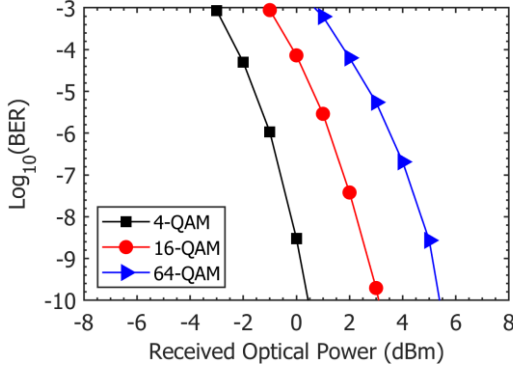


Figure 11. BER against P_r for 20 MHz M -QAM.

IV. CONCLUSIONS

We proposed a hybrid RoF-FSO-PON communications system and presented in simulation using 10 Gb/s 2/4-PAM signals at 40 GHz and a proof-of-concept experimental demonstration using 20 MHz 4/16/64-QAM signals at 25 GHz. Successful transmissions of all signals are achieved with the BER well below 10^{-9} . 4-PAM has been shown to be more robust to the channel impairments compared to 2-PAM. The proposed configuration is simple and capable of reducing the costs of the entire system due to the seamless integration. The proposed concept also provides a solution to deliver high-quality broadband wireless services to remote areas (i.e., last mile problem).

ACKNOWLEDGMENT

This work is supported by International Mobility of Researchers in CTU (CZ.02.2.69/0.0/0.0/16_027/0008465) and MEYS INTER-COST project (within LTC18008).

REFERENCES

- [1] C. Lim, Y. Tian, C. Ranaweera, A. Nirmalathas, E. Wong, and K. Lee, "Evolution of radio-over-fiber technology," *J. Lightwave Technol.*, vol. 37, no. 6, pp. 1647–1656, 2019.
- [2] A. J. Seeds and T. Ismail, "Broadband access using wireless over multimode fiber systems," *J. Lightwave Technol.*, vol. 28, no. 16, pp. 2430–2435, Aug. 2010.
- [3] D.-N. Nguyen *et al.*, "M-QAM transmission over hybrid microwave photonic links at the K-band," *Opt. Express*, vol. 27, no. 23, p. 33745, Nov. 2019.
- [4] D. Novak *et al.*, "Radio-over-fiber technologies for

- emerging wireless systems," *IEEE J. Quantum Electron.*, vol. 52, no. 1, pp. 1–11, 2016.
- [5] A. H. M. R. Islam, M. Bakaul, A. Nirmalathas, and G. E. Town, "Simplified generation, transport, and data recovery of millimeter-wave signal in a full-duplex bidirectional fiber-wireless system," *IEEE Photonics Technol. Lett.*, vol. 24, no. 16, pp. 1428–1430, 2012.
- [6] R. Zhang *et al.*, "An ultra-reliable MMW/FSO A-RoF system based on coordinated mapping and combining technique for 5G and beyond mobile fronthaul," *J. Lightwave Technol.*, vol. 36, no. 20, pp. 4952–4959, Oct. 2018.
- [7] J. Zhang, J. Yu, N. Chi, F. Li, and X. Li, "Experimental demonstration of 24-Gb/s CAP-64QAM radio-over-fiber system over 40-GHz mm-wave fiber-wireless transmission," *Opt. Express*, vol. 21, no. 22, pp. 26888–26895, Nov. 2013.
- [8] K. Kazaura, K. Wakamori, M. Matsumoto, T. Higashino, K. Tsukamoto, and S. Komaki, "RoFSO: A universal platform for convergence of fiber and free-space optical communication networks," *IEEE Commun. Mag.*, vol. 48, no. 2, pp. 130–137, 2010.
- [9] "Free space optics 10 gigabits EL-10G." [Online]. Available: <http://www.ecsystem.cz>.
- [10] C. Ben Naila, K. Wakamori, M. Matsumoto, A. Bekkali, and K. Tsukamoto, "Transmission analysis of digital TV signals over a radio-on-FSO channel," *IEEE Commun. Mag.*, vol. 50, no. 8, pp. 137–144, 2012.
- [11] J. Bohata, S. Zvánovec, P. Pešek, T. Kořínek, M. Abadi, and Z. Ghassemlooy, "Experimental verification of long-term evolution radio transmissions over dual-polarization combined fiber and free-space optics optical infrastructures," *Appl. Opt.*, vol. 55, no. 8, pp. 2109–2116, 2016.
- [12] "5G spectrum GSMA public policy position," 2018. [Online]. Available: <https://www.gsma.com/>.
- [13] ITU-T G.989.1, "40-Gigabit-capable passive optical networks (NG-PON2): General requirements," 2013.
- [14] R. Van Der Linden, N. C. Tran, E. Tangdiongga, and T. Koonen, "Optimization of flexible non-uniform multilevel PAM for maximizing the aggregated capacity in PON deployments," *J. Lightwave Technol.*, vol. 36, no. 12, pp. 2328–2336, 2018.
- [15] Y. Dong, R. P. Giddings, and J. Tang, "Hybrid OFDM-digital filter multiple access PONs," *J. Lightwave Technol.*, vol. 36, no. 23, pp. 5640–5649, 2018.
- [16] A. H. N. Avlonitis, E. M. Yeatman, M. Jones, "Multilevel amplitude shift keying in dispersion uncompensated optical systems," *IET Optoelectron.*, vol. 153, no. 3, pp. 101–108, 2006.
- [17] J. Verbist *et al.*, "40-Gb/s PAM-4 transmission over a 40 km amplifier-less link using a sub-5V Ge APD," *Photonics Technol. Lett.*, vol. 29, no. 24, pp. 2238–2241, 2017.
- [18] 3GPP TS 36.104, "Base station (BS) radio transmission and reception," 2018.